

Cite this: *Nanoscale*, 2023, 15, 3230

## DNA radiosensitization by terpyridine-platinum: damage induced by 5 and 10 eV transient anions†

 Liangde Ouyang,<sup>a</sup> Hong Lin,<sup>a</sup> Puxiang Zhuang,<sup>a</sup> Yu Shao,<sup>a</sup> Meysam Khosravifarsani,<sup>b</sup> Brigitte Guérin,<sup>b</sup> Yi Zheng<sup>\*,a,b</sup> and Léon Sanche<sup>b</sup>

Chemoradiation therapy (CRT), which combines a chemotherapeutic drug with ionizing radiation (IR), is the most common cancer treatment. At the molecular level, the binding of Pt-drugs to DNA sensitizes cancer cells to IR, mostly by increasing the damage induced by secondary low-energy (0–20 eV) electrons (LEEs). We investigate such enhancements by binding terpyridine-platinum (Tpy-Pt) to supercoiled plasmid DNA. Fifteen nanometer thick films of Tpy-Pt–DNA complexes in a molar ratio of 5 : 1 were irradiated with monoenergetic electrons of 5 and 10 eV, which principally attach to the DNA bases to form transient anions (TAs) decaying into a multitude of bond-breaking channels. At both energies, the effective yields of crosslinks (CLs), base damage (BD) related CLs, single and double strand breaks (SSBs and DSBs), non-DSB-cluster lesions, loss of supercoiled configuration and base lesions are  $6.5 \pm 1.5$ ,  $8.8 \pm 3.0$ ,  $88 \pm 11$ ,  $5.3 \pm 1.3$ ,  $9.6 \pm 2.2$ ,  $106 \pm 17$ ,  $189 \pm 31 \times 10^{-15}$  per electron per molecule, and  $11.9 \pm 2.6$ ,  $19.9 \pm 4.4$ ,  $128 \pm 18$ ,  $7.7 \pm 3.0$ ,  $13.4 \pm 3.9$ ,  $144 \pm 19$ ,  $229 \pm 42 \times 10^{-15}$  per electron per molecule, respectively. DNA damage increased 1.2–4.2-fold due to Tpy-Pt, the highest being for BD-related CLs. These enhancements are slightly higher than those obtained by the conventional Pt-drugs cisplatin, carboplatin and oxaliplatin, apart from BD-related CLs, which are about 3 times higher. Enhancements are related to the strong perturbation of the DNA helix by Tpy-Pt, its high dipole moment and its favorable binding to guanine (G), all of which increase bond-breaking *via* TA formation. In CRT, Tpy-Pt could considerably enhance crosslinking within genomic DNA and between DNA and other components of the nucleus, causing roadblocks to replication and transcription, particularly within telomeres, where it binds preferentially within G-quadruplexes.

Received 29th September 2022,  
Accepted 16th January 2023

DOI: 10.1039/d2nr05403e

rsc.li/nanoscale

### 1. Introduction

The combination of high-energy radiation and chemical drugs, called concomitant chemoradiation therapy (CRT), is the most widely used cancer modality to improve treatment efficiency and reduce the toxicity to surrounding healthy tissues.<sup>1–4</sup> Clinical studies have shown that CRT can have a supra-additive effect, *i.e.*, tumor reduction is larger than the sum of chemotherapy and radiation treatment individually.<sup>5–7</sup> In other words, the anti-cancer drug acts simultaneously as a chemotherapeutic agent and a radiosensitizer. Thus, increasing

the effectiveness of either or both properties can improve the clinical outcome of CRT.

Since the discovery of cisplatin ( $\text{Pt}(\text{NH}_3)_2\text{Cl}_2$ ) as a cancer chemotherapeutic agent by Rosenberg in 1965,<sup>8</sup> a variety of platinum(II)-based compounds, including cisplatin, carboplatin and oxaliplatin, have been widely used in CRT.<sup>9–12</sup> The concomitant administration of Pt-drugs and radiation was particularly effective in improving the treatment of non-small cell lung, cervical, head and neck cancers.<sup>13–16</sup> Phase II trials of rectal CRT have shown the feasibility and efficacy of combining oxaliplatin with 5-fluorouracil/folic acid to treat metastatic patients.<sup>17</sup> Despite the wide applications of cisplatin and its derivatives in a variety of cancers, severe side effects have been reported such as neurotoxicity, nephrotoxicity, ototoxicity and retinopathy,<sup>18,19</sup> which could lead to infra-additive results in CRT by Pt-drug administration.<sup>20–22</sup> More worrisome is the intrinsic resistance of cancer cells to these drugs or that acquired during treatment, which limits their applicability<sup>11,23–27</sup> (*e.g.*, colorectal cancers have intrinsic resistance to cisplatin,<sup>28</sup> and chronic resistance to oxaliplatin<sup>29</sup>). It is therefore crucial to develop new chemotherapeutic agents,

<sup>a</sup>State Key Laboratory of Photocatalysis on Energy and Environment, Faculty of Chemistry, Fuzhou University, Fuzhou 350116, P.R. China

<sup>b</sup>Department of Nuclear Medicine and Radiobiology, Faculty of Medicine and Health Sciences, Université de Sherbrooke, Sherbrooke, QC, Canada J1H 5N4.

E-mail: Yi.zheng@usherbrooke.ca

† Electronic supplementary information (ESI) available: Computational docking studies, dosimetry of <sup>64</sup>Cu-NOTA-Tpy-Pt and LEE-induced damage, interduplex crosslinks, UV absorption spectra, exposure–response curves at 5 eV, tables of effective yields for various types of damage in DNA and Pt–drug–DNA complexes. See DOI: <https://doi.org/10.1039/d2nr05403e>

which are strong radiosensitizers and capable of overcoming such resistance, while targeting critical biomolecules with minimum cytotoxicity to normal tissue.<sup>30,31</sup>

In this regard, terpyridine-platinum-II (Tpy-Pt) appears as a promising type of platinum compound. Several groups have characterized *in vitro* binding of Tpy-Pt to DNA quadruplexes and the consequent platination of loops in the human telomeric G-quadruplex. Tpy-Pt comprises a typical planar aromatic ligand of terpyridine (inset of Fig. 1) that can bind covalently to DNA *via* the N7 of guanine (G) bases, as cisplatin does.<sup>32,33</sup> Furthermore, Tpy-Pt has a strong affinity for the three-dimensional DNA structure G-quadruplex (G4).<sup>34–36</sup> It binds preferably to G4, forming a very stable adduct;<sup>34,37</sup> for example, Stafford *et al.* observed for a polypyridyl Tpy-Pt compound a thousand-fold higher affinity toward quadruplexes relative to other DNA sequences.<sup>38</sup> G4 is a quadrilateral stack formed by four Gs, linked together by reverse-Hoogsteen hydrogen bonds associated with the N7 site, which have been

identified as potential targets, particularly in cancer therapy.<sup>39–41</sup> Le Sech and coworkers investigated the radiobiological effect of Tpy-Pt.<sup>42–44</sup> When Tpy-Pt intercalated into supercoiled plasmid DNA (AG30) was irradiated with photons of 11.6 keV, commensurate with the energy of the  $L_{III}$  inner shell of platinum, single-strand and double-strand breaks (SSBs and DSBs) were enhanced. They suggested that atomic Auger electrons emanating from Pt could explain the increase in DNA damage.<sup>42</sup> From irradiation by fast atomic  $He^{2+}$  ions at a linear energy transfer (LET) of 2.24 keV per  $\mu\text{m}$ , similar increase of SSBs and DSBs was observed for Tpy-Pt–DNA complexes, indicating the potential application of Tpy-Pt as a radiosensitizer in radiotherapy.<sup>43</sup> When Chinese hamster ovary cells incubated with 350  $\mu\text{M}$  Tpy-Pt were subsequently irradiated by fast ions  $C^{6+}$  and  $He^{2+}$  with a LET of 2–70 keV per  $\mu\text{m}$ , the cell death rate was increased by a factor of 1.5–2.<sup>44</sup> Despite these results, the compound has never been applied in the clinic. This may reflect the small chemotherapeutic

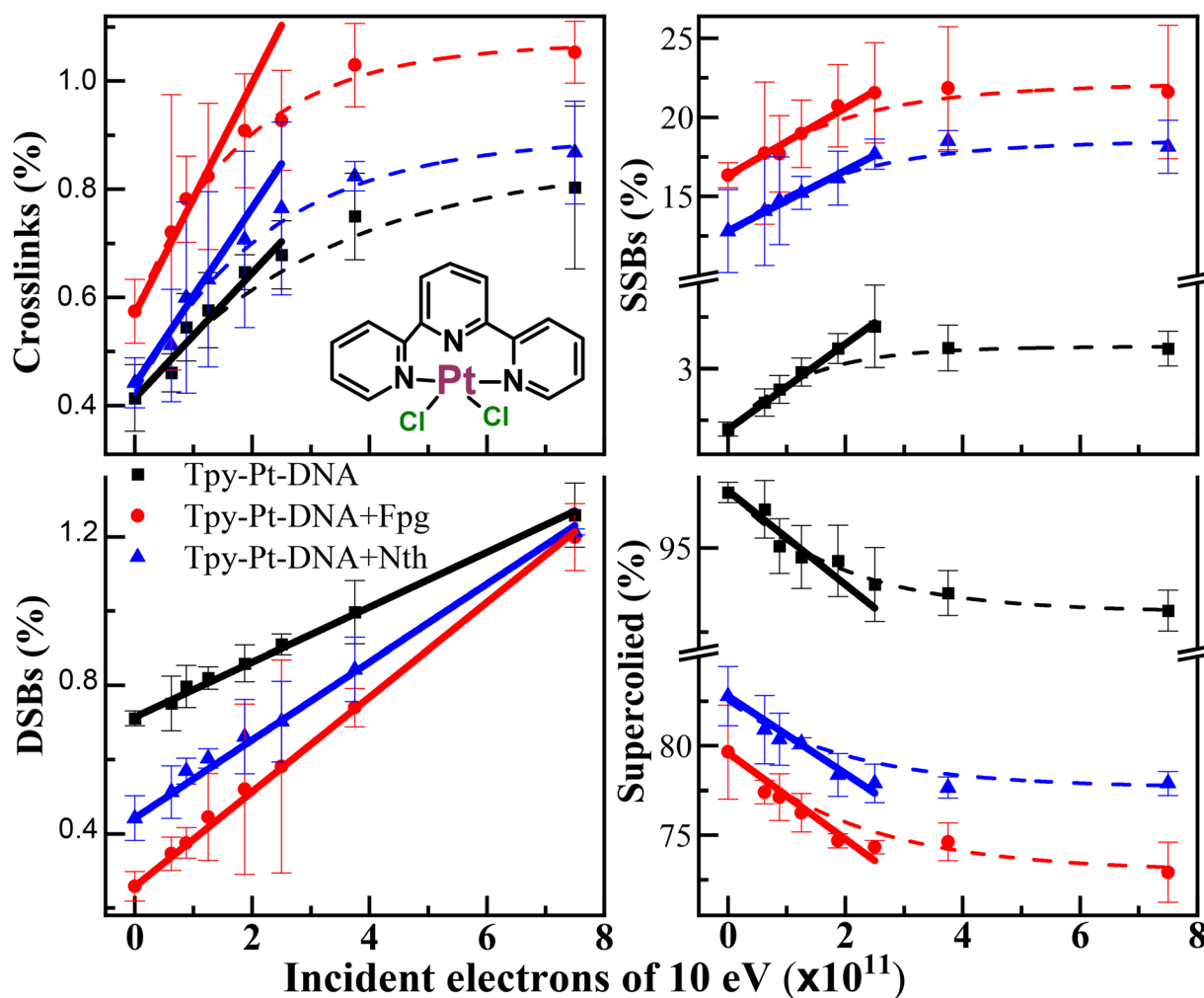


**Fig. 1** Exposure–response curves for DNA damage induced by 10 eV electrons in five-monolayer films of 5 : 1 Tpy-Pt–DNA complexes (■) together with those from parallel treatment by Fpg (●) and Nth (▲) enzymes. The percentages of CLs, SSBs, DSBs and loss of supercoiled DNA are shown in each frame. The structure of Tpy-Pt is shown in the inset. The dashed lines are exponential fits, and the solid lines are linear fits of the initial slopes. The DSBs were fitted with a linear function. Each data point is the result of 10 identical experiments and the error bars are the standard deviations of these measurements.

potential of Tpy-Pt, estimated from the non-toxicity found from *in vivo* studies.<sup>45</sup> However, low toxicity could be an advantage in sparing healthy tissues if Tpy-Pt were to be made highly toxic while present in irradiated cancer cells. This possibility led to more recent experiments.

The cytotoxicity of Tpy-Pt due to its binding with G4 has been shown in two ovarian cancerous cell lines.<sup>36</sup> This specific coordination could induce telomere dysfunction and chromosome instability, indicating suitability of Tpy-Pt compounds as potential chemotherapeutic agents for telomere-targeting therapy.<sup>46</sup> Moreover, since Tpy-Pt derivatives exhibit multiple modes of DNA interactions, as well as inhibit the activity of the epidermal growth factor receptor, they appear as promising multi-targeting anticancer agents.<sup>47</sup> Local radiosensitization by Tpy-Pt has been investigated when conjugated with 1,4,7-triazacyclononane-1,4,7-triacetic acid (NOTA).<sup>48,49</sup> Their cytotoxicity in cancer cells was determined when the conjugates were complexed with either natural or radioactive copper (<sup>64</sup>Cu). Two conjugates were synthesized: Cu-NOTA-Tpy-Pt with a rigid linker and Cu-NOTA-C<sub>3</sub>-Tpy-Pt with a flexible linker.<sup>48,49</sup> <sup>64</sup>Cu-NOTA-Tpy-Pt and <sup>64</sup>Cu-NOTA-C<sub>3</sub>-Tpy-Pt resulted, respectively, in a >27 800-fold and 55 000-fold increase of cytotoxicity for P53-wild type colorectal cancer cells HCT116, compared to their non-radioactive Tpy-Pt counterparts under the same conditions.<sup>48,49</sup> These huge enhancements in cell death were principally attributed to a combination of the action of the short-range Auger electrons emitted from <sup>64</sup>Cu and the ability of Tpy-Pt to intercalate at sensitive sites in the DNA of HCT116 cells, particularly within the G4 structures. In addition, chemotherapeutic enhancements of 2.7 and 4 were respectively obtained at 24 h and 72 h post administration of <sup>64</sup>Cu-NOTA-Tpy-Pt, indicating the possibility of local CRT.<sup>48</sup> Hence, the continued development of Tpy-Pt, and related conjugates, as a radiosensitizer and potential chemotherapeutic agent in CRT could benefit from a more detailed understanding of the radiosensitization mechanism at the molecular level.

Generally, radiosensitization by Pt-chemotherapeutic drugs has been related to an increase of cellular platinum uptake, enhancement of DNA damage and inhibition of DNA repair, leading to cell cycle arrest.<sup>12,50–54</sup> In *in vitro* and *in vivo* studies, repair of DNA damage was inhibited by the synergistic administration of cisplatin and radiation.<sup>55–58</sup> At the molecular level, the binding of Pt-drugs to DNA sensitizes the molecule to ionizing radiation, increasing the damage induced by the secondary reactive species, particularly those caused by secondary low energy (0–20 eV) electrons (LEEs).<sup>59,60</sup>

When high-energy primary particles interact with biological media, copious quantities of secondary LEEs are generated by ionization.<sup>61,62</sup> These electrons play a crucial role in inducing radiobiological damage in cells,<sup>63,64</sup> which effectively causes genotoxic damage, *e.g.*, detrimental DNA lesions.<sup>65–67</sup> The enhancement of LEE-induced DNA damage resulting from the binding of radiosensitizers provides a basis for the molecular mechanism of action in CRT.<sup>59,68–76</sup> In the case of Pt-drugs, this mechanism has been verified *in vitro* and *in vivo*, as optimal CRT could be achieved when the amount of the Pt-

drug is at the maximum in the nucleus of the cancer cells.<sup>77–80</sup> These studies showed the pertinence of understanding the radiosensitization of LEE-induced damage by Pt-agents, in providing valuable information for developing novel Pt-analogues and improving guidelines for CRT protocols. In particular, such information was useful in the development of the previously mentioned <sup>64</sup>Cu-NOTA-Tpy-Pt conjugates, for which the radioisotope <sup>64</sup>Cu was chosen as a copious source of LEEs.<sup>48</sup> <sup>64</sup>Cu emits Auger electrons of 840 eV, which along their short path (~50 nm) produce a high density of LEEs having a range of about 10 nm. Moreover, the positrons of 0.655 MeV emitted by <sup>64</sup>Cu can serve to locate the conjugate by positron emission tomography. So far, the interaction of LEEs with Tpy-Pt–DNA complexes has not been investigated.

The present experiments are performed with plasmids extracted from *E. coli* DH5, which have supercoiled configurations and contain guanine enriched sequences that form G4.<sup>81,82</sup> These eukaryotic plasmids contain configurations similar to the DNA found in human mitochondria.<sup>83</sup> Furthermore, their supercoiled structure and length provide a suitable model for investigating ionizing radiation damage to genomic DNA.<sup>67</sup> G4 structures can be formed in both bacterial DNA (*e.g.*, *E. coli*)<sup>84</sup> and human cell nuclei.<sup>85</sup> While G4s play a crucial role for genomic stability and cell viability in both eukaryotes and prokaryotes, they represent only a very small fraction (*i.e.*, about 1%) of the human and bacterial genome.<sup>82,84,86</sup> Nevertheless, the affinity of terpyridine platinum compounds towards G4s is 1000-fold higher than it is towards the native form of DNA.<sup>36,38</sup> For this reason, we consider here the binding of Tpy both to common base configurations and to G4s.

In unmodified DNA, the electron energy dependence of the yields (*i.e.*, the yield function) for the formation of SSBs, DSBs, BDs, non-DSB cluster damage and crosslinks (CLs) exhibits maxima around 5–6 and 10 eV. These yields are mainly the result of an initial electron capture by the bases leading to the formation of transient anions (TAs), decaying into bond-breaking processes.<sup>65–67</sup> Herein, we investigate the influence of binding Tpy-Pt to DNA on the lesions induced by these TAs, which dominate the damage cross sections near 5 and 10 eV.<sup>67,72</sup> The binding of Tpy-Pt to DNA is characterized by inductively coupled plasma mass spectroscopy and UV spectrophotometry. The effective yields of the damage induced to non-modified plasmids are compared to that induced to Tpy-Pt–plasmid complexes from respective fluence–response curves. Enhancement factors (EFs) vary from 1.2 to 4.2, depending on the type of damage, with BD-related CLs being the highest. The results are discussed in relation to mechanisms that could be implicated in Tpy-Pt radiosensitization to LEE-induced damage in mitochondrial and genomic DNA.

## 2. Experimental section

### 2.1. Preparation and characterization of terpyridine-Pt–DNA complexes

Plasmid DNA [pGEM-3Zf(–), 3197 base pairs (bp)] was extracted from *E. coli* DH5 and purified with a HiSpeed

plasmid giga kit (QIAGEN), as previously described.<sup>87,88</sup> The extracted DNA consisted of 96.3% of the supercoiled configuration, 2.0% concatemeric, 0.8% nicked circular and 0.9% CLs. Dichloro (2,2':6',2''-terpyridine) platinum(II) dihydrate (Tpy-Pt) was purchased from Sigma-Aldrich with a purity of 99.0% and used without further purification.

Tpy-Pt dissolved in distilled deionized water (ddH<sub>2</sub>O) was mixed with the plasmids and incubated in the dark at room temperature for 2 h. The solution was passed through a Sephadex G-50 column to isolate Tpy-Pt–DNA complexes and remove the buffer and free Tpy-Pt. The standard curve of Pt<sup>2+</sup> counts correlated to Tpy-Pt concentrations was characterized by inductively coupled plasma mass spectroscopy. The binding efficiency of Tpy-Pt to DNA was determined to be 75% from the ratio of Pt<sup>2+</sup> counts after and before passing through the G-50 column. Tpy-Pt–DNA complexes were prepared with a molar ratio of 5 : 1. This ratio was chosen to maximize the yields, while avoiding any overlap of the perturbations caused by Tpy-Pt within DNA. The absorption spectra of Tpy-Pt, DNA and Tpy-Pt–DNA solutions were measured by ultraviolet-visible diffuse reflectance spectroscopy (UV-Vis DRS) to reflect the extent of variation of the electronic state of Tpy-Pt after binding with DNA.

## 2.2. LEE irradiation

Seven  $\mu\text{L}$  of Tpy-Pt–DNA ddH<sub>2</sub>O solution containing 320 ng of DNA was deposited on clean tantalum substrates, where they were lyophilized to produce thin films of  $2.0 \pm 0.5$  mm radius. Taking  $1.7 \text{ g cm}^{-3}$  as the film density,<sup>72</sup> the average thickness of the films corresponded to 15 nm ( $\sim 5$  monolayers). The films were transferred into the ultra-high vacuum chamber of a LEE irradiator, which had been evacuated for 24 h. During bombardment of the samples, the potential between the substrate (ground) and the center of the filament of the LEE gun was set at 5.4 and 10.4 eV. By subtracting from these values, for the 0.4 V potential measured for the threshold of electron arrival at the substrate, the absolute electron energies were 5 and 10 eV. The electron beam current was set at 2 nA giving a current density of  $10^{11}$  electron per  $\text{cm}^2$  per s. To generate the exposure–response curves (*i.e.*, yields of different DNA configurations *vs.* fluence), samples were exposed to the beam for 5, 7, 10, 15, 20, 30 and 60 s, respectively. At each period, ten samples were irradiated, while 4 samples were maintained in vacuum without irradiation as controls. After each irradiation cycle, the Tpy-Pt–DNA films were recovered from the Ta substrates using 20  $\mu\text{L}$  of ddH<sub>2</sub>O.

## 2.3. Enzyme treatment and quantification of DNA conformation variations

The recovered irradiated and control samples were divided into three portions: two of them were treated with *E. coli* base excision repair endonuclease III (Nth) and formamidopyrimidine *N*-glycosylase (Fpg), respectively, to reveal base modifications, as described previously.<sup>72</sup> Samples treated with the latter were separately incubated at 37 °C for 60 min. The plasmid constituents in all portions corresponding to super-

coiled, nicked circular, linear and CLs were analyzed by 1% agarose gel electrophoresis and quantified by the ImageQuant 5.0 (Molecular Dynamics) software.<sup>87</sup> When recorded from the non-treated samples, these conformations corresponded to intact DNA, SSBs, DSBs and inter-plasmid CLs, respectively. The conformational modifications arising from enzyme treatment served to quantitate the BD, non-DSB cluster damage and BD-related CLs. The measured CLs induced by electron irradiation without enzyme treatment correspond to prompt strand breaks leading to interduplex chemical bonds, whereas the BD-related CLs occur when the endonucleases cleave at the site of the damaged nucleotide, leaving a strand break.<sup>89</sup> Consequently, the radical formed reacts with its surroundings yielding an interduplex or interstrand CL. The process is similar to nucleotide excision repair in the cell.<sup>90</sup> As previously mentioned by Dong *et al.*, crosslinks within a DNA strand could be recognized by both endonucleases as types of base modifications and transformed into a DSB.<sup>67</sup>

## 2.4. Effective yields of plasmid damage

The effective yields of DNA damage were obtained by extrapolating the slope of the exposure–response curves to zero fluence. Because of the low cross reactivity of Nth and Fpg for enzyme-sensitive sites, the enzyme-sensitive sites (ess) recognized by both enzymes were considered independent.<sup>89</sup> As Fpg and Nth enzymes specifically identify the BD of purine and pyrimidine,<sup>90</sup> the corresponding yields for the two different BD-related lesions could be differentiated as  $Y(\text{Fpg})_{\text{pur}}$  and  $Y(\text{Nth})_{\text{pyr}}$ , respectively. Accordingly, the sum of the base lesions  $Y(\text{base lesion})_{\text{ess}}$  that caused a given DNA damage were obtained as follows:

$$Y(\text{base lesion})_{\text{ess}} = Y(\text{Nth})_{\text{pyr}} + Y(\text{Fpg})_{\text{pur}} - 2[Y(\text{DNA}) + Y(\text{heat})],$$

where  $Y(\text{DNA})$  represents the yields of DNA damage in the absence of enzyme treatments and  $Y(\text{heat})$  the yield of heat labile sites, arising from the DNA samples incubated at 37 °C for 60 min without enzymes.<sup>72</sup> The total yields of DNA damage are given by<sup>91</sup>

$$Y(\text{total}) = Y(\text{Nth})_{\text{pyr}} + Y(\text{Fpg})_{\text{pur}} - Y(\text{DNA}) - 2Y(\text{heat}).$$

# 3. Results and discussion

## 3.1. Binding of Tpy-Pt to DNA

The interactions of Tpy-Pt with DNA is quite distinct from those of traditional platinum-based compounds due to the favored intercalation of the flat Tpy-Pt structure within G4 configurations *via* weak  $\pi$ – $\pi$  interactions.<sup>33,36</sup> Being bifunctional, Tpy-Pt can still form interstrand and intrastrand CLs within the DNA helix, most likely between guanines, adenines or both,<sup>92,93</sup> as do cisplatin, carboplatin and oxaliplatin,<sup>9–11</sup> although monofunctional binding to G is also possible.<sup>46,94</sup> Tpy-Pt and Tpy-based complexes interact with the quadruplex configuration *via* three major pathways: firstly, by  $\pi$ – $\pi$  interactions with two opposing faces of a G4; secondly, by direct



intercalation into the lateral and diagonal loops of G4s and finally, through replacement of monovalent alkaline ions, which usually fill the central channels of three-dimensional G4s.<sup>34,38</sup> Furthermore, it has been clearly demonstrated that Tpy-Pt selectively coordinates into certain adenines (*i.e.*, A7 and A13) of a telomere-like quadruplex structure located in the loop.<sup>32,34</sup>

Further theoretical insight into the molecular interaction between Tpy-Pt and B-DNA can be gained by computational docking studies. To this end, the optimal structure of Tpy-Pt was docked with B-DNA, taken from the protein data bank, using the HDock server.<sup>95</sup> Further details are given in the ESI, where Fig. 1S† shows that Tpy-Pt binds within the major groove of DNA, mainly *via* hydrophobic  $\pi$ -sigma and  $\pi$ - $\pi$  interaction with G and A bases. The interaction of Tpy-Pt within the major groove was also reported by Suntharalingam *et al.* for Tpy-based compounds that induce apoptosis.<sup>96</sup> Moreover, the Tpy-Pt-DNA complex was found to be essentially unaltered by the present manipulations, indicating that it could be slightly more stable than those formed with cisplatin, carboplatin and oxaliplatin (ESI Table 2S†).

UV-visible absorption spectra of different sample solutions are provided in Fig. 2S of the ESI.† The spectra include those of solutions of unreacted Tpy-Pt, purified Tpy-Pt-DNA from passing through the Sephadex column, and purified Tpy-Pt-DNA bombarded by 10 eV electrons for 30 s. The spectra of Tpy-Pt-DNA complexes before and after removal of salts, and electron-irradiation are similar to those of the absorption peak of unreacted DNA, exhibiting a strong absorption maximum at 260 nm.<sup>97</sup> Thus, any changes in electronic structure of DNA, due to the binding of five Tpy-Pt molecules to the 3197 base-pair plasmids, do not modify UV-visible absorption under any of the conditions investigated. Tpy-Pt has three characteristic absorption peaks at 248, 278 and 336 nm as shown in Fig. 2S.†<sup>98</sup> The first two are not visible from absorption by Tpy-Pt-DNA, since they strongly overlap the spectrum of DNA. However, the 336 nm peak, which is attributed to charge-transfer transitions from Pt to Tpy can be resolved;<sup>99</sup> it is observed at the same wavelength in solutions containing only Tpy-Pt and in those containing purified Tpy-Pt-DNA, irradiated or not with LEEs. Thus, the structure of terpyridine seems to remain intact, probably reflecting the weak binding of Tpy-Pt to DNA, *via*  $\pi$ -sigma and  $\pi$ - $\pi$  interactions, as projected from docking computations (ESI†). Moreover, since the spectrum of irradiated Tpy-Pt remains unaffected by irradiation, we can conjecture that LEEs do not break bonds within the cyclic structure of terpyridine and only cleave the Pt-N7 (guanine or adenine) bonds when they exist.

Compared to the common Pt-drugs, Tpy forms a bulkier adduct with DNA. The molecular weight in  $\text{g mol}^{-1}$  of Tpy-Pt (535) is 1.3–1.7-fold higher than that for oxaliplatin (397), carboplatin (371), and cisplatin (301). The difference is larger after hydrolysis and coordination to DNA. Therefore, the bending, and unwinding pattern generated in the Tpy-Pt-DNA helix should be larger than that induced by cisplatin, oxaliplatin and carboplatin. For example, DNA unwinding created by

cisplatin is about 13 degrees,<sup>100</sup> but the corresponding value for Tpy-Pt-DNA is about 20 degrees.<sup>37</sup> Thus, as the physico-chemical characteristics of bonds in proximity of Tpy-Pt-DNA adducts should be more strongly modified than in conventional Pt-drugs, the electron-resonance scattering characteristics are expected to change accordingly.

### 3.2. Yields of damage to Tpy-Pt-DNA induced by 5 and 10 eV electrons

Each exposure–response curve in Fig. 1 shows the percentage variation of CLs, SSBs, DSBs and the supercoiled configuration, as a function of 10 eV electron fluence, with or without treatment with Fpg and Nth enzymes. Each data point is the result of ten independent experiments with films of Tpy-Pt-DNA. Similar curves resulting from 5 eV electron impact are provided in the ESI.† The exposure–response curves of Tpy-Pt-DNA exhibit similar trends as those induced by LEE impact on other Pt-drug-DNA complexes.<sup>59,72,101</sup> In Fig. 1, the curves for SSBs and supercoiled DNA display similar magnitudes, indicating that supercoiled DNA primarily converts into the nicked circular configuration (SSBs). For supercoiled DNA, SSBs and CLs, the curves show a similar exponential behavior as a function of fluence. Since initial targets available to produce the linear forms (DSBs) are much more slowly depleted as the fluence increases (*i.e.*, both SSBs and supercoiled DNA are initial sources for DSB formation), the yields of DSBs *vs.* fluence fit a linear function.<sup>102</sup>

Each effective yield for a given DNA damage per incident electron-molecule corresponds to the sum of the damage created by the impact of a single electron of a given energy.<sup>102</sup> They are obtained by dividing the initial slopes of the respective fluence–response curves by the percentage of supercoiled DNA at zero fluence. Fig. 2 presents a histogram of the yields of each type of damage induced by 5 and 10 eV electron impact on Tpy-Pt-DNA and DNA films of 5 monolayers under identical conditions. The histogram includes directly produced conformational damage and those related to BDs revealed by enzyme treatment. The yields induced by 10 eV electrons are higher than those produced at 5 eV, as expected from the larger extent of TA states at 10 eV. Consistently, the yields from Tpy-Pt-DNA are larger than those of unmodified DNA, demonstrating that the binding of Tpy-Pt to the plasmids increases appreciably LEE-induced damage. The latter are enhanced differently depending on the type of damage and electron energy. The numerical values of these yields are listed in Table 1S of the ESI,† where they are compared to the results previously obtained under identical conditions, with cisplatin, carboplatin and oxaliplatin bound to DNA.<sup>59,72,101,103</sup>

### 3.3. Damage increases induced by Tpy-Pt and other Pt-drugs relative to unmodified DNA

The enhancement factor (EF), defined as the ratio of the yield of a specific damage to DNA bound to a Pt-compound to that without the Pt-drug is usually considered to be a suitable parameter to estimate and compare the sensitization efficacies of different Pt-analogues.<sup>59,60,72,101</sup> The EFs resulting from the

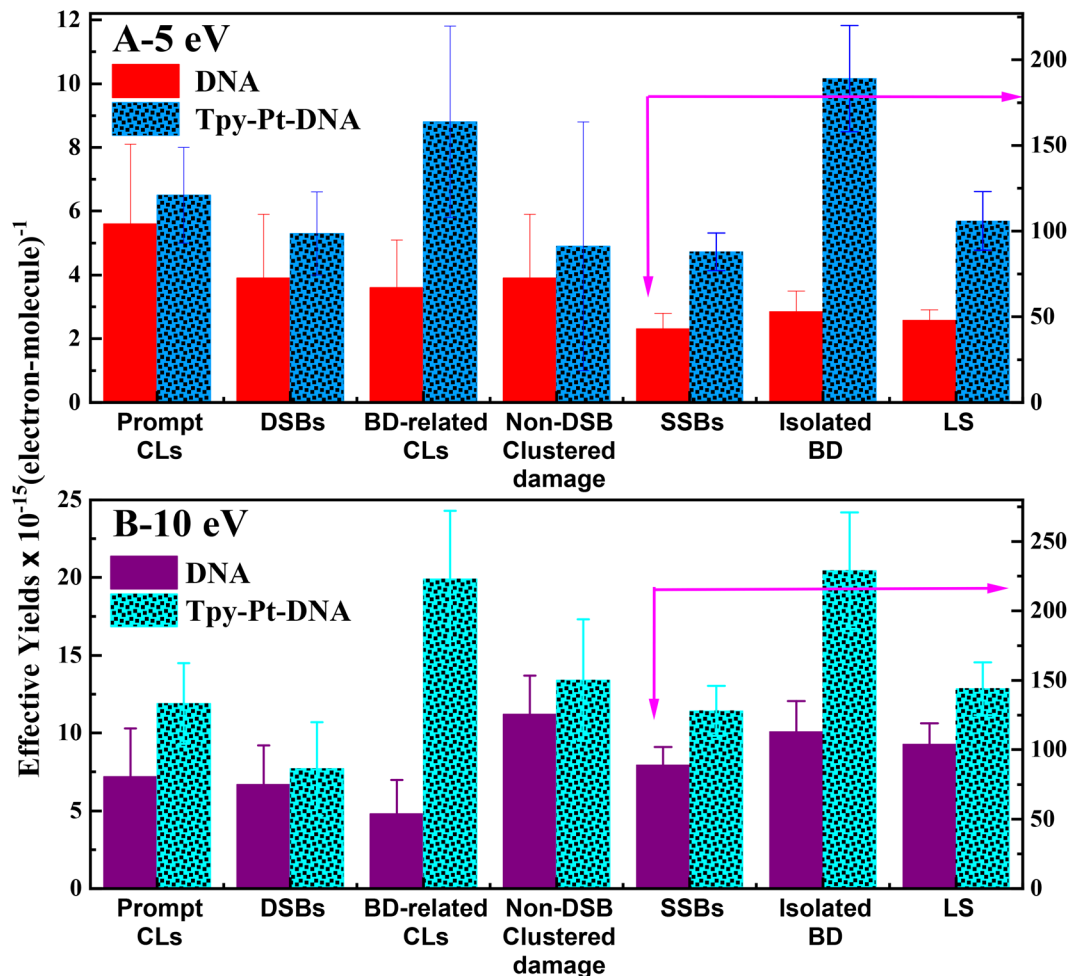


Fig. 2 The effective yields in electron per molecule of DNA damage including CLs, SSBs, DSBs, loss of supercoiled (LS) DNA and BD related lesions for Tpy-Pt-DNA complexes and DNA induced by 5 (A) and 10 eV (B) electrons. The errors are calculated from a linear regression fit analysis of the slope of respective exposure response curves near zero fluence.

binding of Tpy-Pt to DNA inferred from the 5 and 10 eV yields of Fig. 2 are listed in Table 1 (in the order of increasing values for the first line). The known EFs at those energies of other Pt-drugs also appear in this table. All EFs are larger than 1, indicating pervasive radiosensitization with the four Pt-compounds. For Tpy-Pt-DNA, the EFs at 5 eV are usually higher than those generated by 10 eV electrons.

Generally, the EFs of Tpy-Pt are similar to those of the traditional Pt-chemotherapeutic agents. As for the DSBs and non-DSB cluster damage, the three traditional Pt-drugs display higher and similar EFs, respectively, compared to those obtained with Tpy-Pt. Although the EFs of the total yields of damage are similar for all four Pt-drugs, the type of lesion is modulated differently. For example, Tpy-Pt produces an EF of  $4.2 \pm 2.1$  for BD-related CLs at 10 eV, whereas for the other Pt-drugs this EFs lie much lower, *i.e.*, in the range 1.4–1.7. The detailed comparison of purine- and pyrimidine-related damage induced by 10 eV electrons in Pt-drug-DNA complexes is shown in Fig. 3,<sup>72,103</sup> where the yields of purine-related damage are found to be larger than those related to pyrimi-

dine. However, the enhancement varies for different Pt-compounds and DNA damage. *Clearly, Tpy-Pt considerably enhances purine-related CLs compared to the other three Pt-drugs.*

The EFs and the data of Fig. 2 and 3 suggest that LEEs interacting with Tpy-Pt-DNA have a propensity to attach to purine bases to form TAs that decay preferentially into bond-breaking processes leading to base damage and related CLs. This finding most likely reflects the favorable binding of Tpy to purines, which are known to produce higher damage yields *via* TA formation.<sup>72</sup> *Compared to other Pt-DNA complexes, the larger deformation and opening of the helix caused by Tpy-Pt could favor (1) the modification of resonance parameters (i.e., the lifetime, energy, decay channels and electron capture and transfer probability of the TAs), and (2) CL formation by exposing a larger surface to adjacent molecules.* Some of the hypotheses advanced in this paragraph are substantiated by different types of experiments by other groups.

Rackwitz and Bald reported a higher LEE damage cross section for telomere sequences of DNA relative to other intermixed DNA sequences.<sup>104</sup> This was explained by the proximity

**Table 1** The comparison of the enhancement factors (EFs) of DNA damage for various Pt-drugs obtained by 5 and 10 eV electron impact. The EF is defined as the yield of a given damage in the Pt–DNA complex divided by that in nonmodified DNA under identical conditions. The EFs of Tpy–Pt–DNA induced by 5 eV electrons are listed in order of increasing values from left to right in the first line

Electron energy (eV)	Target	Prompt CLs	Non-DSB cluster damage	DSBs	SSBs	Loss of supercoiled	BD-related CLs	Isolated BD	Total BDs	Total damage
5	Tpy–Pt–DNA	1.2 ± 0.6	1.3 ± 1.2	1.4 ± 0.8	2.1 ± 0.4	2.2 ± 0.5	2.4 ± 1.3	<b>3.6 ± 1.0</b>	2.5 ± 1.0	2.4 ± 0.8
	Cisplatin–DNA <sup>72</sup>	1.4 ± 0.2	1.6 ± 1.3	1.7 ± 0.3	1.4 ± 0.2	1.4 ± 0.4	2.5 ± 1.4	2.4 ± 0.7	2.4 ± 1.1	2.1 ± 1.1
10	Tpy–Pt–DNA	1.7 ± 0.8	1.2 ± 0.4	1.2 ± 0.6	1.4 ± 0.3	1.4 ± 0.3	<b>4.2 ± 2.1</b>	2.0 ± 0.5	2.3 ± 0.8	1.9 ± 0.6
	Cisplatin–DNA <sup>60</sup>	2.2 ± 0.9		2.5 ± 0.4	1.4 ± 0.4					
	Carboplatin–DNA <sup>60</sup>	3.1 ± 1.0		3.1 ± 0.5	1.5 ± 0.4					
	Oxaliplatin–DNA <sup>60</sup>	4.1 ± 1.8		2.4 ± 0.4	1.5 ± 0.4					
	Cisplatin–DNA <sup>72</sup>	1.4 ± 1.0	1.4 ± 0.5	1.4 ± 0.7	1.4 ± 0.4	1.7 ± 0.4	1.4 ± 0.9	1.7 ± 0.5	1.9 ± 0.4	1.8 ± 0.3
	Cisplatin–DNA <sup>103</sup>	2.4 ± 0.8	1.4 ± 0.5	1.5 ± 0.3	1.5 ± 0.2	1.5 ± 0.2	1.7 ± 1.1	1.4 ± 0.8	1.9 ± 0.9	1.7 ± 0.4
	Carboplatin–DNA <sup>103</sup>	1.7 ± 0.4	1.1 ± 0.4	1.9 ± 0.4	1.3 ± 0.2	1.3 ± 0.2	1.6 ± 0.7	1.3 ± 0.6	1.6 ± 0.6	1.4 ± 0.3
	Oxaliplatin–DNA <sup>103</sup>	1.8 ± 0.4	1.4 ± 0.5	1.4 ± 0.3	1.7 ± 0.2	1.7 ± 0.2	1.5 ± 0.6	2.3 ± 0.7	2.6 ± 0.9	2.1 ± 0.5

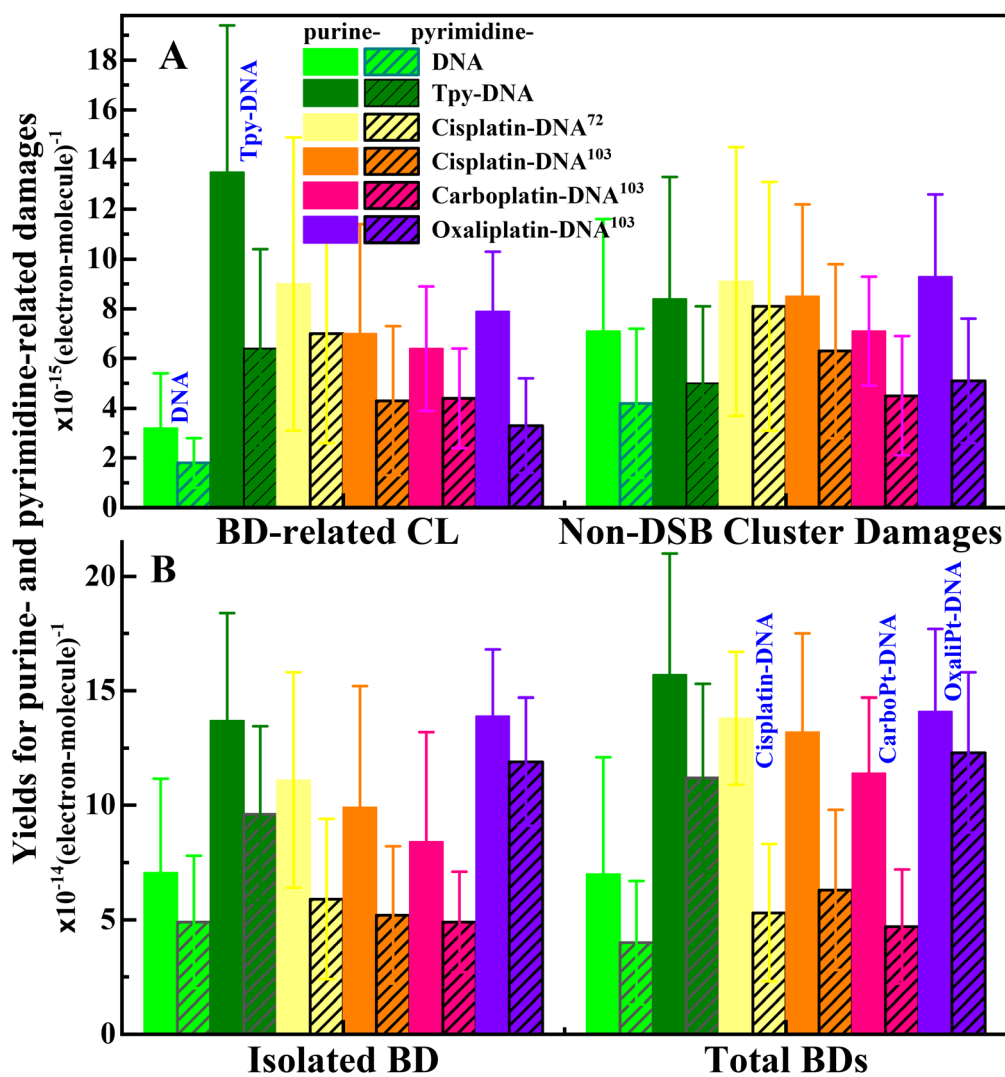


**Fig. 3** Comparison of yields for purine- and pyrimidine-related damage induced by 10 eV electrons, which were detected by Fpg and Nth enzyme treatment, respectively. The yields for cisplatin, carboplatin and oxaliplatin are unpublished results taken from the data bank used to obtain the sum of the purine and pyrimidine yields given in the cited papers.

of adenine and guanine bases, which capture electrons more effectively and increase damage by a factor of about 7.5 compared to that in controls.<sup>104</sup> In tumor cells, Merle *et al.* found a significant increase in DSBs, telomere dysfunction induced foci and telomere deletions, after combination treatment with Tpy-Pt and external beam radiation therapy, relative to Tpy-Pt treatment and radiation therapy alone.<sup>105</sup> The enhanced cytotoxicity for conjugation of <sup>64</sup>Cu and NOTA-Tpy-Pt at the cellular level,<sup>48</sup> relative to radiolabeling with cisplatin<sup>106</sup> in combination with external beam radiation therapy also supports our hypotheses. DNA radiosensitization in HTC116 colorectal cancer cells by <sup>64</sup>Cu-NOTA-C<sub>3</sub>-Tpy-Pt and <sup>64</sup>Cu-NOTA-Tpy-Pt, is derived from two mechanisms: (1) the displacement of the protective Shelterin complex and/or hindrance of telomerase activity on telomeres by Tpy-Pt residues and (2) disruption of G4 structure by LEEs emitted from <sup>64</sup>Cu.<sup>48</sup> Further information on the relationship between the damage induced by LEEs in HTC116 colorectal cancer cells and <sup>64</sup>Cu-NOTA-Tpy-Pt compounds is provided in the ESI.†

In LEE experiments with plasmid films, bond cleavage results in a radical that can form intrastrand or interduplex CLs. Thus, the magnitude of the detectable interduplex CLs reported herein could serve as a guideline to estimate cross-linking in the cell nucleus, where intrastrand, interstrand and DNA-protein CLs are specific categories of DNA damage, which require sophisticated cellular checkpoints and repair pathways.<sup>107</sup> From a biological point of view, this type of damage can be seen as analogous to the end-to-end fusion of two adjacent chromosomes (or chromatid), which is considered to be highly detrimental to cell viability.<sup>108</sup> Interstrand CLs are considered to be the most cytotoxic among all cross-linking lesions, causing a covalent roadblock to replication and transcription.<sup>109</sup> CLs are more challenging for the cell to repair than other individual, widely dispersed lesions, and regarded to be lethal carcinogens or mutagens.<sup>107</sup> The preferred induction of CLs by Tpy-Pt indicates that it could act as an efficient radiosensitizer.

### 3.4. TAs of DNA and DNA-Pt-drug complexes and their decay channels

In unmodified duplex DNA and oligonucleotides, TAs are formed at 5 and 10 eV in the yield functions of single damage.<sup>110</sup> In the yield functions of cluster damage, they occur at 6 and 10 eV.<sup>110</sup> These TAs are of the core-excited types (*i.e.*, two-electron one-hole states) caused by the incident electron being temporarily captured into an unfilled molecular orbital with simultaneous excitation of another electron from a ground-state orbital into a higher-energy empty one. In other words, the electron is captured by the positive electron affinity of an electronically excited state of a nucleotide.<sup>72</sup> The numerous decay channels of these resonances are well established and have been discussed in detail in previous papers.<sup>72,110–115</sup> Within DNA, a core-excited TA is usually formed on a base, where it can decay *via* autoionization or DEA.<sup>67,87,110</sup> In the latter case, a BD is produced, which can include base release. Following autoionization, the emitted electron can transfer to

the phosphate group, where DEA can produce a SSB.<sup>66,67,87</sup> Production of more complex damage with a single electron is also possible, if the autoionizing electron leaves the base in an electronically excited state, which dissociates and hence induces a BD.<sup>67</sup> Then, the escaping electron can transfer to another fundamental unit in the same or opposite strand, where it can form a second TA, decaying *via* DEA and producing further damage. The possible combinations of double lesions include two BDs, a BD + SSB lesions and a DSB, if a BD is later converted into a strand break. According to ongoing time dependent DFT calculations,<sup>116</sup> triple lesions caused by the formation of a single core-excited anion state on a base are also possible, if the two excited electrons of the core excited TA autoionize to transfer and induce DEA at two other sites. In this case, a third lesion can result from the reaction of the cationic site formed within DNA.

Since the discovery that LEEs play a significant role in CRT, the damage induced by the decay of the 5–6 and 10 eV TAs has been investigated with DNA bound to the traditional Pt-drugs.<sup>59,60,72,101</sup> These TAs cause strong maxima in the damage yield functions. The most detailed analysis is found in the work of Dong *et al.*,<sup>117</sup> who generated yield functions for all types of measurable damage in plasmid DNA and *cis*-Pt-DNA complexes, as well as consistently positive EFs within the entire 1–20 eV range.<sup>101,117</sup> Despite the perturbation of cisplatin, the resonance peaks appeared at 5–6 and 10 eV in both cases, within the resolution of their experiment ( $\pm 0.5$  eV). Thus, they concluded that same or similar TAs were involved whether cisplatin was present or not. The reason for this behavior may be simply that the binding of cisplatin does not change the resonance energy sufficiently for the energy difference between modified and non-modified DNA to be resolvable experimentally. It could also be related to the fact that resonance maxima in yield functions occur at the energy of the first interaction. Since there is only one cisplatin out of 1279 bases in DNA-cisplatin complexes, in most cases, electrons should first be captured at an unperturbed site and hence bear the signature of the original DNA yield function. After its formation, the TA dissociates or autoionizes. In the latter case, the additional electron is likely to be injected into the DNA conduction band, where it could travel some distance to be finally trapped into the deeper well of a binding site of cisplatin. According to the calculations of Caron *et al.*,<sup>118–122</sup> this distance could be of the order of 10 base pairs. The transfer would reduce the emitted electron probability to escape the DNA molecule and lead to further damage (*i.e.*, EF > 1), favored by the stronger electron capture at the cisplatin site. We expect a similar behavior with Tpy-DNA complexes, *i.e.*, the measured EFs reflect an enhancement of the magnitude of the decay channels of the 5–6 and 10 eV TAs leading to bond scission.

### 3.5. Radiosensitization mechanism of Tpy-Pt: binding to purines and resonance parameters

In this section, we consider electron capture at or near the binding site of Tpy. The electron can arrive from inside or



outside DNA, probably with different probabilities of being captured. Within the regions perturbed by Tpy, we expect the processes described in the previous section to be modified in proportion to the perturbation. A priori, mono or bifunctional binding of Tpy-Pt is possible to any base, but it is expected to preferentially intercalate within G4 regions or other regions containing adenines with Gs, or only adenines.<sup>32,33</sup> Such intercalations should modify the resonance parameters in their vicinity.

In the case of *cis*-Pt–DNA, covalent bonding of Pt to the N7 position of the purine bases causes unwinding and bending of the double helix toward the major groove.<sup>9,11</sup> This results in a wider minor groove, weakening the strength of the bonds and improving the accessibility of LEEs to the bases near the site of platination; such modifications could extend over twenty bp.<sup>123</sup> In Tpy-Pt–DNA complexes, due to the larger size and mass of Tpy-Pt, these modifications are expected to extend over even larger distances and hence influence the resonance parameters of TAs of a larger number of bases, which are all highly dependent on the immediate environment.<sup>124–126</sup> This perturbation should lead to an increase of magnitude of DEA and electron transfer, thus enhancing damage yields. Particularly, the presence of Pt<sup>2+</sup>, could lower the TA energy. Although this energy shift could be too small to be perceived in a yields function, as it was the case for cisplatin–DNA complexes, it should decrease the number of decay channels and thus increase the resonance lifetime. Since the DEA yields depend exponentially on this lifetime,<sup>126</sup> the modification should increase the EFs, even if there are only 5 Tpy-Pt conjugates on average bound to plasmids containing 3197 bp, *i.e.*, one Tpy out of 1279 bases. Considering charge transfer or a perturbation extending along 20 bp, there are 320 (~5%) bases in a modified environment that could be reached by an incoming or transferred electron. Consequently, an EF of 2 for a particular damage translates into an average enhancement of DEA by a factor of 20 in the perturbed region. Such a modification is quite reasonable and much smaller than that observed with environmental changes around some simple molecules.<sup>124,125</sup>

In the interaction of LEEs with Tpy-Pt–DNA involving interstrand and intrastrand covalent bounds with two Gs, the electron is more likely to be initially captured by a G. The TA thus formed can subsequently dissociate causing cleavage of the Pt–G bond, either leaving the electron stabilized on the base or on the Tpy-Pt moiety, most likely reducing the metal to Pt<sup>+</sup>. The electron capture by guanine bound to Tpy-Pt can lead to DEA, producing either a BD, CL, DSB or non-DSB cluster damage.<sup>117</sup> In addition to crosslinking, a diversity of reactions with guanine radicals exist, among which the most prominent is base release.<sup>127,128</sup> Considering the integrity of terpyridine after electron bombardment, suggested from the UV-Vis absorption spectrum (Fig. 1S†), the resulting G radicals could (1) follow the oxidation and/or reduction processes causing guanine-BDs and (2) abstract hydrogen from the backbones, leading to the cleavage of phosphodiester bonds, *i.e.*, BD + SSB.<sup>129</sup> Since the self-assembly of guanine-rich motifs are mainly located on telomeres and oncogene promoters,<sup>41</sup> the

preferable binding of Tpy-Pt with these critical targets should promote radiosensitization of tumor cells during radiotherapy.

From recent calculations, performed on the cytosine nucleotide, it has been suggested that dipole-bound (DB) TAs could serve as a doorway to electron capture into valence orbitals of the bases and the phosphate group of DNA.<sup>130</sup> As shown for simpler molecules,<sup>131–140</sup> a DB TA is formed when the incoming electron is first captured into a diffuse DB state *via* deposition of its energy in vibrational degrees of freedom of the target molecule, thus forming a vibrational Feshbach resonance.<sup>131,141,142</sup> If the DB anion is coupled to a valence state, the electron can transfer into a more compact orbital. Coupling of DB states to core-excited TAs has recently been observed in DEA to gaseous formamide and its methylated derivatives, *N*-methylformamide and *N,N*-dimethylformamide, as well as in electron photodetachment from the pyrazolide anion.<sup>143,144</sup> We therefore mention the possibility of formation of a DB state, although the existence of such a doorway mechanism remains to be extended to, not only aqueous environment,<sup>145</sup> but also long DNA strands. According to the calculations in the ESI,† using the Marvin Sketch software (version 21.15),<sup>146</sup> the dipole moment of hydrolyzed Tpy-Pt is 8.03 Debye, whereas for oxaliplatin and cisplatin/carboplatin, it is 5.4 and 1.48 Debye, respectively (Tpy-Pt > oxaliplatin > cisplatin/carboplatin). The hydrolyzed conditions were chosen because these Pt-based compounds must be hydrolyzed to interact with DNA (*i.e.*, the chlorine ion or other leaving groups are replaced by water molecules during the preparation with dd H<sub>2</sub>O). Usually, dipole anion states become quasi-bound when the permanent dipole moment of the neutral molecule, is greater than 2.5 D.<sup>147–149</sup> Thus, the calculated values make oxaliplatin and Tpy-Pt candidates for the doorway mechanism, with Tpy-Pt providing the strongest electron-dipole interaction. However, due to the periodicity of nucleotides in relatively long DNA strands, LEEs tend first, to diffract along these quasi-equally spaced basic DNA constituents, as shown theoretically by Caron and coworkers.<sup>118–122</sup> From this perspective, it appears unlikely that an incoming LEE would initially localize on a specific fundamental DNA constituent, unless the periodic symmetry were broken. Such a break inevitably occurs by the inclusion of another molecule, such as a Pt-drug, within the DNA double helix. This situation could create more favorable conditions for the formation of DB states that could act as a doorway to a more localized core-excited TA. In any case, the dipole moment of Tpy-Pt should contribute to the potential binding of the electron to Tpy, during the formation of core-excited TAs.

## 4. Conclusions

We measured the yields of various lesions induced by 5 and 10 eV electrons to Tpy-Pt–DNA complexes at a ratio of 5 : 1. These lesions include SSBs, DSBs, BDs, CLs and non-DSB cluster damage. The chosen DNA (*i.e.*, Eukaryotic plasmids) contains configurations similar to those found in human mitochondria,

and its supercoiled structure and length provide a suitable model for the investigation of genomic DNA damage induced by ionizing radiation.<sup>67,150</sup>

At 5 and 10 eV, bond dissociation occurs mostly *via* the formation of core-excited TAs decaying into DEA, or autoionization when the target site is left in a dissociative state. From the present investigation, we find that enhancement factors for all specific damage are larger than one, with the highest one being observed for BD-related CLs ( $4.2 \pm 2.1$ ). The yields of BDs as a percentage of the total damage are 63% and 65% at each energy, respectively. Although the total damage yields in Tpy-Pt-DNA complexes are similar to those of the conventional Pt-drugs (*i.e.*, cisplatin, carboplatin and oxaliplatin), a much larger number of BDs and CLs is induced by binding Tpy-Pt to DNA; such damage is mostly found on the purine bases. Compared to conventional Pt-drugs, this marked difference could result from three factors: (1) the preferred binding of Tpy-Pt to guanine bases, particularly within G4 configurations, (2) the larger size of Tpy-Pt, which favors a larger perturbation and opening of the helix and (3) the stronger dipole moment of Tpy-Pt. The contribution of the first factor is easily explained from electron attachment to guanine above 5 eV, which leads to the highest damage yields among all bases.<sup>104</sup> Compared to other Pt-drugs, the larger size of Tpy-Pt is expected to (1) further modify the parameters of core-excited TAs, producing larger damage yields and (2) amplify covalent binding of the induced radicals to other DNA molecules in the films, thus considerably enhancing the yields of CLs. Finally, the higher dipole moment of Tpy-Pt could favor the formation of dipole bound states. The latter have been shown to serve as a doorway to the formation of core-excited TAs, which are responsible for the greatest damage seen in the present experiment. Since the self-assembly of guanine-rich motifs mainly locate on telomeres and oncogene promoters,<sup>41</sup> the preferable binding of Tpy-Pt with these critical targets in cells is expected to promote radiosensitization during external beam radiotherapy and targeted radionuclide therapy.

## Author contributions

L. O., H. L., and P. Z. designed and performed the experimental work. L. O. and P. Z. analyzed the data. Y. S. coordinated the project. B. G., Y. Z. and L. S. provided financial support and expertise. L. O., M. K., Y. Z., and L. S. wrote the manuscript. All the authors have approved the final version of the manuscript after the discussion.

## Conflicts of interest

The authors declare no competing financial interest.

## Acknowledgements

Financial support for this work was provided by the Canadian Institutes of Health Research (PJT-162325), the Natural Science

and Engineering Research Council of Canada (RGPIN-2018-14882) and the National Natural Science Foundation of China (21673044). We are indebted to Dr Andrew D. Bass and Prof. Richard Wagner for their critical comments.

## References

- G. D. Wilson, S. M. Bentzen and P. M. Harari, *Semin. Radiat. Oncol.*, 2006, **16**, 2–9.
- T. Y. Seiwert, J. K. Salama and E. E. Vokes, *Nat. Clin. Pract. Oncol.*, 2007, **4**, 86–100.
- H. Choy, *Chemoradiation in cancer therapy*, Humana Press, Tennessee, 2003.
- V. T. Devita, T. S. Lawrence and S. A. Rosenberg, *Cancer: Principles and practice of oncology*, Lippincott Williams & Wilkins, New York, 2001.
- P. J. Eifel, *Nat. Clin. Pract. Oncol.*, 2006, **3**, 248–255.
- M. Candelaria, A. Garcia-Arias, L. Cetina and A. Duenas-Gonzalez, *Radiat. Oncol.*, 2006, **1**, 1.
- P. Boscolo-Rizzo, A. Gava, C. Marchiori, V. Baggio and M. C. Da Mosto, *Ann. Oncol.*, 2011, **22**, 1894–1901.
- B. Rosenberg, L. V. Camp and T. Krigas, *Nature*, 1965, **205**, 698–699.
- Y. Jung and S. J. Lippard, *Chem. Rev.*, 2007, **107**, 1387–1407.
- L. Kelland, *Nat. Rev. Cancer*, 2007, **7**, 573–584.
- T. C. Johnstone, K. Suntharalingam and S. J. Lippard, *Chem. Rev.*, 2016, **116**, 3436–3486.
- S. Nagasawa, J. Takahashi, G. Suzuki, Y. Hideya and K. Yamada, *Int. J. Mol. Sci.*, 2021, **22**, 3140.
- J. Jassem, *Lancet Oncol.*, 2001, **2**, 335–342.
- P. G. Rose, *Eur. J. Cancer*, 2002, **38**, 270–278.
- G. P. Browman, D. I. Hodson, R. J. Mackenzie, N. Bestic and L. Zuraw, *Head Neck-J. Sci. Spec.*, 2001, **23**, 579–589.
- X. Le and E. Y. Hanna, *Ann. Transl. Med.*, 2018, **6**, 229.
- G. Freyer, N. Bossard, P. Romestaing, F. Mornex, O. Chapet, V. Trillet-Lenoir and J. Gérard, *J. Clin. Oncol.*, 2001, **19**, 2433–2438.
- T. Boulikas and M. Vougiouka, *Oncol. Rep.*, 2003, **10**, 1663–1682.
- S. Dasari and P. B. Tchounwou, *Eur. J. Pharmacol.*, 2014, **740**, 364–378.
- A. C. Begg, *Int. J. Radiat. Oncol., Biol., Phys.*, 1990, **19**, 1183–1189.
- M. Candelaria, A. Garcia-Arias, L. Cetina and A. Duenas-Gonzalez, *Radiat. Oncol.*, 2006, **1**, 15–31.
- Y. Asaka-Amano, Y. Takiguchi, M. Yatomi, K. Kurosu, Y. Kasahara, N. Tanabe, K. Tatsumi and T. Kuriyama, *Radiat. Res.*, 2007, **167**, 637–644.
- P. Pil and S. J. Lippard, Cisplatin and related drugs, in *Encyclopedia of Cancer*, ed. J. R. Bertino, Academic Press, New York, 2nd edn, 2002, pp. 525–543.
- F.-S. Liu, *Taiwan. J. Obstet. Gynecol.*, 2009, **48**, 239–244.
- J. Karges, T. Yempala, M. Tharaud, D. Gibson and G. Gasser, *Angew. Chem., Int. Ed.*, 2020, **59**, 7069–7075.

- 26 D. Shen, L. M. Pouliot, M. D. Hall and M. M. Gottesman, *Pharmacol. Rev.*, 2012, **64**, 706–721.
- 27 M. Ashrafizadeh, A. Zarrabi, K. Hushmandi, F. Hashemi, E. R. Moghadam, M. Owrang, F. Hashemi, P. Makvandi, M. A. S. B. Goharrizi, M. Najafi and H. Khan, *Cellular Signalling*, 2021, **78**, 109871.
- 28 D. W. Shen, S. Goldenberg, I. Pastan and M. M. Gottesman, *J. Cell. Physiol.*, 2000, **183**, 108–116.
- 29 A. D. Yang, F. Fan, E. R. Camp, G. V. Buren, W. Liu, R. Somcio, M. J. Gray, H. Cheng, P. M. Hoff and L. M. Ellis, *Clin. Cancer Res.*, 2006, **12**, 4147–4153.
- 30 L. K. Kvols, *J. Nucl. Med.*, 2005, **46**, 187S–190S.
- 31 J. L. Barnes, M. Zubair, K. John, M. C. Poirier and F. L. Martin, *Biochem. Soc. Trans.*, 2018, **46**, 1213–1224.
- 32 H. Bertrand, S. Bombard, D. Monchaud, E. Talbot, A. Guedin, J.-L. Mergny, R. Grunert, P. Bednarskid and M.-P. Teulade-Fichou, *Org. Biomol. Chem.*, 2009, **7**, 2864–2871.
- 33 K. Suntharalingam, A. J. P. White and R. Vilar, *Inorg. Chem.*, 2009, **48**, 9427–9435.
- 34 S. N. Georgiades, N. H. Abd Karim, K. Suntharalingam and R. Vilar, *Angew. Chem., Int. Ed.*, 2010, **49**, 4020–4034.
- 35 Z. Ou, Y. Wang, Y. Gao, X. Wang, Y. Qian, Y. Li and X. Wang, *J. Inorg. Biochem.*, 2017, **166**, 126–134.
- 36 E. Morel, C. Beauvineau, D. Naud-Martin, C. Landras-Guetta, D. Verga, D. Ghosh, S. Achelle, F. Mahuteau-Betzer, S. Bombard and M.-P. Teulade-Fichou, *Molecules*, 2019, **24**, 404.
- 37 S. D. Cummings, *Coord. Chem. Rev.*, 2009, **253**, 1495–1516.
- 38 V. S. Stafford, K. Suntharalingam, A. Shivalingam, A. J. P. White, D. J. Mann and R. Vilar, *Dalton Trans.*, 2015, **44**, 3686–3700.
- 39 S. Neidle, *J. Med. Chem.*, 2016, **59**, 5987–6011.
- 40 S. Müller and R. Rodriguez, *Expert Rev. Clin. Pharmacol.*, 2014, **7**, 663–679.
- 41 R. Hänsel-Hertsch, M. D. Antonio and S. Balasubramanian, *Nat. Rev. Mol. Cell Biol.*, 2017, **18**, 279–284.
- 42 C. L. Sech, K. Takakura, C. Saint-Marc, H. Frohlich, M. Charlier, N. Usami and K. Kobayashi, *Can. J. Physiol. Pharmacol.*, 2001, **79**, 196–200.
- 43 N. Usami, Y. Furusawa, K. Kobayashi, H. Frohlich, S. Lacombe and C. Lesech, *Int. J. Radiat. Biol.*, 2005, **81**, 515–522.
- 44 N. Usami, Y. Furusawa, K. Kobayashi, S. Lacombe, A. Reynaud-Angelin, E. Sage, T.-D. Wu, A. Croisy, J.-L. Guerquin-Kern and C. Lesech, *Int. J. Radiat. Biol.*, 2008, **84**, 603–611.
- 45 D. M. Fisher, R. R. Fenton and J. R. Aldrich-Wright, *Chem. Commun.*, 2008, **43**, 5613–5615.
- 46 N. Petrov, H.-S. Lee, M. Liskovych, M.-P. Teulade-Fichou, H. Masumoto, W. C. Earnshaw, Y. Pommier, V. Larionov and N. Kouprina, *Oncotarget*, 2021, **12**, 1444–1456.
- 47 C. Li, F. Xu, Y. Zhao, W. Zheng, W. Zeng, Q. Luo, Z. Wang, K. Wu, J. Du and F. Wang, *Front. Chem.*, 2020, **8**, 210.
- 48 M. Khosravifarsani, S. Ait-Mohand, B. Paquette, L. Sanche and B. Guérin, *J. Med. Chem.*, 2021, **64**, 6765–6776.
- 49 M. Khosravifarsani, S. Ait-Mohand, B. Paquette, L. Sanche and B. Guérin, *Nanomaterials*, 2021, **11**, 2154.
- 50 R. C. Richmond, *Radiat. Res.*, 1984, **99**, 596–608.
- 51 G. P. Amorino, M. L. Freeman, D. P. Carbone, D. E. Lebowitz and H. Choy, *Int. J. Radiat. Oncol., Biol., Phys.*, 1999, **44**, 399–405.
- 52 L.-X. Yang, E. B. Double and H. J. Wang, *Int. J. Radiat. Oncol., Biol., Phys.*, 1995, **33**, 641–646.
- 53 T. Servidei, C. Ferlini, A. Riccardi, D. Mecco, G. Scambia, G. Segni, C. Manzotti and R. Riccardi, *Eur. J. Cancer*, 2001, **37**, 930–938.
- 54 N. J. Morel, M. Illand, Y. T. Kim, J. Paul and R. Brown, *Cancer Res.*, 1999, **59**, 2102–2106.
- 55 L. Dewit, *Int. J. Radiat. Oncol., Biol., Phys.*, 1987, **13**, 403–426.
- 56 J. D. Zimbrick, A. Sukrochana and R. C. Richmond, *Int. J. Radiat. Oncol., Biol., Phys.*, 1979, **5**, 1351–1354.
- 57 P. Lelieveld, M. A. Scoles, J. M. Brown and R. F. Kallman, *Int. J. Radiat. Oncol., Biol., Phys.*, 1985, **11**, 111–121.
- 58 I. Munaweera, Y. Shi, B. Koneru, R. Saez, A. Aliev, A. J. Di Pasqua and K. J. Balkus, *Mol. Pharmaceutics*, 2015, **12**, 3588–3596.
- 59 Y. Zheng, D. J. Hunting, P. Ayotte and L. Sanche, *Phys. Rev. Lett.*, 2008, **100**, 198101.
- 60 M. Rezaee, D. J. Hunting and L. Sanche, *Int. J. Radiat. Oncol., Biol., Phys.*, 2013, **87**, 847–853.
- 61 J. A. LaVerne and S. M. Pimblott, *Radiat. Res.*, 1995, **141**, 208–215.
- 62 S. M. Pimblott and J. A. Laverne, *Radiat. Phys. Chem.*, 2007, **76**, 1244–1247.
- 63 S. Kouass Sahbani, P. Cloutier, A. D. Bass, D. J. Hunting and L. Sanche, *J. Phys. Chem. Lett.*, 2015, **6**, 3911–3914.
- 64 S. Kouass Sahbani, L. Sanche, P. Cloutier, A. D. Bass and D. J. Hunting, *J. Phys. Chem. B*, 2015, **118**, 13123–13131.
- 65 E. Alizadeh and L. Sanche, *Chem. Rev.*, 2012, **112**, 5578–5602.
- 66 E. Alizadeh, T. M. Orlando and L. Sanche, *Annu. Rev. Phys. Chem.*, 2015, **66**, 379–398.
- 67 Y. Dong, Y. Gao, W. Liu, T. Gao, Y. Zheng and L. Sanche, *J. Phys. Chem. Lett.*, 2019, **10**, 2985–2990.
- 68 C. J. McGinn, D. S. Shewach and T. S. Lawrence, *J. Natl. Cancer Inst.*, 1996, **88**, 1193–1203.
- 69 L. Sanche, *Chem. Phys. Lett.*, 2009, **474**, 1–6.
- 70 M. Rezaee, E. Alizadeh, P. Cloutier, D. J. Hunting and L. Sanche, *ChemMedChem*, 2014, **9**, 1145–1149.
- 71 M. Zdrowowicz, L. Chomicz, M. Zyndul, P. Wityk, J. Rak, T. J. Wiegand, C. G. Hanson, A. Adhikary and M. D. Sevilla, *Phys. Chem. Chem. Phys.*, 2015, **17**, 16907–16916.
- 72 Y. Dong, L. Zhou, Q. Tian, Y. Zheng and L. Sanche, *J. Phys. Chem. C*, 2017, **121**, 17505–17513.
- 73 R. Schürmann, S. Vogel, K. Ebel and I. Bald, *Chem. – Eur. J.*, 2018, **24**, 10271–10279.

- 74 J. Ameixa, E. Arthur-Baidoo, R. Meißner, S. Makurat, W. Kozak, K. Butowska, F. F. da Silva, J. Rak and S. Denifl, *J. Chem. Phys.*, 2018, **149**, 164307.
- 75 R. Meißner, S. Makurat, W. Kozak, P. Limão-Vieira, J. Rak and S. Denifl, *J. Phys. Chem. B*, 2019, **123**, 1274–1282.
- 76 M. Zdrowowicz, P. Spisz, A. Hac, A. Herman-Antosiewicz and J. Rak, *Int. J. Mol. Sci.*, 2022, **23**, 1429.
- 77 T. Tippyamontri, R. Kotb, B. Paquette and L. Sanche, *Anticancer Res.*, 2012, **32**, 4395–4404.
- 78 T. Tippyamontri, R. Kotb, B. Paquette and L. Sanche, *Anticancer Res.*, 2013, **33**, 3005–3014.
- 79 T. Tippyamontri, R. Kotb, L. Sanche and B. Paquette, *Anticancer Res.*, 2014, **34**, 5303–5312.
- 80 G. Charest, T. Tippyamontri, M. Shi, M. Wehbe, M. Anantha, M. Bally and L. Sanche, *Int. J. Mol. Sci.*, 2020, **21**, 4848.
- 81 M. Falabella, J. E. Kolesar, C. Wallace, D. de Jesus, L. Sun, Y. V. Taguchi, C. Wang, T. Wang, I. M. Xiang, J. K. Alder, R. Maheshan, W. Horne, J. Turek-Herman, P. J. Pagano, C. M. St. Croix, N. Sondheimer, L. A. Yatsunyk, F. B. Johnson and B. A. Kaufman, *Sci. Rep.*, 2019, **9**, 5605.
- 82 V. J. Parekh, B. A. Niccum, R. Shah, M. Rivera, M. J. Novak, F. Geinguenaud, F. Wien, V. Arluison and R. Sinden, *Microorganisms*, 2020, **8**, 28.
- 83 K. Boguszewska, M. Szewczuk, J. Kaźmierczak-Barańska and B. T. Karwowski, *Molecules*, 2020, **25**, 2857.
- 84 W. M. Guiblet, M. DeGiorgio, X. Cheng, F. Chiaromonte, K. A. Eckert, Y. F. Huang and K. D. Makova, *Genome Res.*, 2021, **31**, 1136–1149.
- 85 A. V. Pavlova, E. A. Kubareva, M. V. Monakhova, M. I. Zvereva and N. G. Dolinnaya, *Biomolecules*, 2021, **11**, 1284.
- 86 R. Y. Wu, K. W. Zheng, J. Y. Zhang, Y. H. Hao and Z. Tan, *Angew. Chem., Int. Ed.*, 2015, **54**, 2447–2451.
- 87 X. Luo, Y. Zheng and L. Sanche, *J. Chem. Phys.*, 2014, **140**, 155101.
- 88 X. Chen, N. Karmaker, P. Cloutier, A. Bass, Y. Zheng and L. Sanche, *J. Phys. Chem. B*, 2022, **126**, 5443–5457.
- 89 A. Yokoya, S. M. T. Cunniffe and P. O'Neill, *J. Am. Chem. Soc.*, 2002, **124**, 8859–8866.
- 90 C. J. Burrows and J. G. Muller, *Chem. Rev.*, 1998, **98**, 1109–1152.
- 91 Y. Shao, Y. Dong, D. Hunting, Y. Zheng and L. Sanche, *J. Phys. Chem. C*, 2017, **121**, 2466–2472.
- 92 C. S. Peyratout, T. K. Aldridge, D. K. Crites and D. R. McMillin, *Inorg. Chem.*, 1995, **34**, 4484–4489.
- 93 J. Li, R. Liu, J. Jiang, X. Liang, G. Huang, D. Yang, H. Chen, L. Pan and Z. Ma, *J. Inorg. Biochem.*, 2020, **210**, 111165.
- 94 G. Zhu, M. Myint, W. H. Ang, L. Song and S. J. Lippard, *Cancer Res.*, 2012, **7**, 790–800.
- 95 Y. Yan, H. Tao, J. He and S.-Y. Huang, *Nat. Protoc.*, 2020, **15**, 1829–1852.
- 96 K. Suntharalingam, O. Mendoza, A. A. Duarte, D. J. Mann and R. Vilar, *Metalomics*, 2013, **5**, 514–523.
- 97 T. Yagura, K. Makita, H. Yamamoto, C. F. M. Menck and A. P. Schuch, *Sensors*, 2011, **11**, 4277–4294.
- 98 G. Annibale, M. Brandolisio and B. Pitteri, *Polyhedron*, 1995, **14**, 451–453.
- 99 E. Marie, A. Ratilla, H. Brothers II and N. Kostic, *J. Am. Chem. Soc.*, 1987, **109**, 4592–4599.
- 100 H. Loskotová and V. Brabec, *Eur. J. Biochem.*, 1999, **266**, 392–402.
- 101 Q. Bao, Y. Chen, Y. Zheng and L. Sanche, *J. Phys. Chem. C*, 2014, **118**, 15516–15524.
- 102 M. Rezaee, P. Cloutier, A. D. Bass, M. Michaud, D. J. Hunting and L. Sanche, *Phys. Rev. E: Stat., Nonlinear, Soft Matter Phys.*, 2012, **86**, 031913.
- 103 Y. Cai, L. Zhou, Y. Gao, W. Liu, Y. Shao and Y. Zheng, *ChemistrySelect*, 2019, **4**, 1084–1091.
- 104 J. Rackwitz and I. Bald, *Chem. – Eur. J.*, 2018, **24**, 4680–4688.
- 105 P. Merle, M. Gueugneau, M. Teulade-Fichou, M. Müller-Barthélémy, S. Amiard, E. Chautard, C. Guetta, V. Dedieu, Y. Communal, J. Mergny, M. Gallego, C. White, P. Verrelle and A. Tchirkov, *Sci. Rep.*, 2015, **5**, 16255.
- 106 J. Areberg, A. Johnsson and J. Wennerberg, *Int. J. Radiat. Oncol., Biol., Phys.*, 2000, **46**, 1275–1280.
- 107 A. Sancar, L. A. Lindsey-Boltz, K. Unsal-Kacmaz and S. Linn, *Annu. Rev. Biochem.*, 2004, **73**, 39–85.
- 108 A. D. Bolzán, *Mutagenesis*, 2012, **27**, 1–15.
- 109 H. B. Rycenga and D. T. Long, *Curr. Opin. Pharmacol.*, 2018, **41**, 20–26.
- 110 Y. Zheng and L. Sanche, *Int. J. Mol. Sci.*, 2019, **20**, 3749.
- 111 G. J. Schulz, *Rev. Mod. Phys.*, 1973, **45**, 423–486.
- 112 R. E. Palmer and P. J. Rous, *Rev. Mod. Phys.*, 1992, **64**, 383–440.
- 113 M. Allan, *J. Electron Spectrosc. Relat. Phenom.*, 1989, **48**, 219–351.
- 114 H. Hotop, M.-W. Ruf, M. Allan and I. I. Fabrikant, *Adv. At., Mol., Opt. Phys.*, 2003, **49**, 85–216.
- 115 L. Sanche, Primary Interactions of Low Energy Electrons in Condensed Matter, in *Excess Electrons in Dielectric Media*, ed. J.-P. Jay-Gerin and C. Ferradini, CRC Press, Boca Raton, 1991, pp. 1–42.
- 116 M. D. Sevilla, L. Sanche, D. Becker, A. Kumar and A. Adhikary, *Abstracts of the 65th Annual meeting of the Radiation Research Society*, San Diego, Nov. 2019.
- 117 Y. Dong, Y. Wang, P. Zhuang, X. Fu, Y. Zheng and L. Sanche, *J. Phys. Chem. B*, 2020, **120**, 3315–3325.
- 118 L. Caron and L. Sanche, *Phys. Rev. Lett.*, 2003, **91**, 113201.
- 119 L. Caron and L. Sanche, *Phys. Rev. A*, 2004, **70**, 032719.
- 120 L. Caron and L. Sanche, *Phys. Rev. A*, 2006, **73**, 062707.
- 121 L. Caron and L. Sanche, *Phys. Rev. A*, 2005, **72**, 032726.
- 122 L. Caron, L. Sanche, S. Tonzani and C. H. Greene, *Phys. Rev. A*, 2009, **80**, 012705.
- 123 E. R. Jamieson and S. J. Lippard, *Chem. Rev.*, 1999, **99**, 2467–2498.
- 124 L. Sanche, A. D. Bass, P. Ayotte and I. I. Fabrikant, *Phys. Rev. Lett.*, 1995, **75**, 3568–3571.



- 125 K. Nagesha and L. Sanche, *Phys. Rev. Lett.*, 1998, **81**, 5892–5896.
- 126 E. Alizadeh, S. Ptasińska and L. Sanche, Transient Anions in Radiobiology and Radiotherapy: From Gaseous Biomolecules to Condensed Organic and Biomolecular Solids, in *Radiation Effects in Materials*, IntechOpen, London, 2016, pp. 180–230.
- 127 S. Choofong, P. Cloutier, L. Sanche and J. R. Wagner, *Radiat. Res.*, 2016, **186**, 520–530.
- 128 D. Angelov, I. N. Lone, H. Menoni and J. Cadet, *Photochem. Photobiol.*, 2022, **98**, 662–670.
- 129 M. Dizdaroglu and P. Jaruga, *Free Radical Res.*, 2012, **46**, 382–419.
- 130 S. J. J. Narayanan, D. Tripathi and A. K. Dutta, *J. Phys. Chem. Lett.*, 2021, **12**, 10380–10387.
- 131 T. Sommerfeld, *J. Phys.: Conf. Ser.*, 2005, **4**, 245–250.
- 132 V. K. Voora and K. D. Jordan, *J. Phys. Chem. A*, 2014, **118**, 7201–7205.
- 133 J. P. Rogers, C. S. Anstoter and J. R. R. Verlet, *Nat. Chem.*, 2018, **10**, 341–346.
- 134 M. A. Yandell, S. B. King and D. M. Neumark, *J. Am. Chem. Soc.*, 2013, **135**, 2128–2131.
- 135 J. P. Rogers, C. S. Anstoter and J. R. R. Verlet, *J. Phys. Chem. Lett.*, 2018, **9**, 2504–2509.
- 136 J. N. Bull and J. R. R. Verlet, *Sci. Adv.*, 2017, **3**, e1603106.
- 137 J. N. Bull, C. W. West and J. R. R. Verlet, *Chem. Sci.*, 2016, **7**, 5352–5361.
- 138 F. Lecomte, S. Carles, C. Desfrancois and M. A. Johnson, *J. Chem. Phys.*, 2000, **113**, 10973–10977.
- 139 J. H. Hendricks, S. A. Lyapustina, H. L. de Clercq and K. H. Bowen, *J. Chem. Phys.*, 1998, **108**, 8–11.
- 140 M. E. Castellani, C. S. Anstoter and J. R. R. Verlet, *Phys. Chem. Chem. Phys.*, 2019, **21**, 24286–24290.
- 141 J. P. Gauyacq and A. Herzenberg, *Phys. Rev. A*, 1982, **25**, 2959–2967.
- 142 G. A. Gallup and I. I. Fabrikant, *Phys. Rev. A*, 2011, **83**, 012706.
- 143 Z. Li, M. Ryszka, M. M. Dawley, I. Carmichael, K. B. Bravaya and S. Ptasińska, *Phys. Rev. Lett.*, 2019, **122**, 073002.
- 144 Y.-R. Zhang, D.-F. Yuan and L.-S. Wang, *J. Phys. Chem. Lett.*, 2022, **13**, 2124–2129.
- 145 I. Anusiewicz, P. Skurski and J. Simons, *J. Phys. Chem. A*, 2020, **124**, 2064–2076.
- 146 Biovia, *Discovery Studio Modeling Environment (Release 4.5)*, Dassault Systèmes, San Diego, 2015.
- 147 K. D. Jordan and F. Wang, *Annu. Rev. Phys. Chem.*, 2003, **54**, 367–396.
- 148 J. Simons, *J. Phys. Chem. A*, 2008, **112**, 6401–6511.
- 149 O. H. Crawford and W. R. Garrett, *J. Chem. Phys.*, 1977, **66**, 4968–4970.
- 150 E. Coutinho, C. Batista, F. Sousa, J. Queiroz and D. Costa, *Mol. Pharmaceutics*, 2017, **14**, 626–638.